Title

Selective cannabinoid-1 receptor blockade benefits fatty acid and triglyceride metabolism significantly in weight-stable nonhuman primates

Journal

AJP Endocrinology and Metabolism, 303(5)

ISSN

0193-1849

Authors

Vaidyanathan, Vidya
Bastarrachea, Raul A
Higgins, Paul B
et al.

Publication Date

2012-09-01

DOI

10.1152/ajpendo.00072.2012

Am J Physiol Endocrinol Metab 303: E624–E634, 2012.
First published July 3, 2012; doi:10.1152/ajpendo.00072.2012.

Selective cannabinoid-1 receptor blockade benefits fatty acid and triglyceride metabolism significantly in weight-stable nonhuman primates

Vidya Vaidyanathan,[1]* Raul A. Bastarrachea,[2]* Paul B. Higgins,[6] V. Saroja Voruganti,[2] Subhash Kamath,[3] Nicholas V. DiPatrizio,[4] Daniele Piomelli,[4,5] Anthony G. Comuzzie,[2] and Elizabeth J. Parks[1]

[1]*Center for Human Nutrition, University of Texas Southwestern Medical Center, Dallas, Texas;* [2]*Department of Genetics, Texas Biomedical Research Institute, San Antonio, Texas;* [3]*Department of Medicine/Division of Diabetes, University of Texas Health Science Center at San Antonio, San Antonio, Texas;* [4]*Department of Pharmacology, University of California-Irvine School of Medicine, Irvine, California;* [5]*Unit of Drug Discovery and Development, Italian Institute of Technology, Genoa, Italy; and* [6]*Center for Laboratory Animal Sciences, Crown Bioscience at the David H. Murdock Research Institute, Kannapolis, North Carolina*

Submitted 7 February 2012; accepted in final form 27 June 2012

Vaidyanathan V, Bastarrachea RA, Higgins PB, Voruganti VS, Kamath S, DiPatrizio NV, Piomelli D, Comuzzie AG, Parks EJ. Selective cannabinoid-1 receptor blockade benefits fatty acid and triglyceride metabolism significantly in weight-stable nonhuman primates. *Am J Physiol Endocrinol Metab* 303: E624–E634, 2012. First published July 3, 2012; doi:10.1152/ajpendo.00072.2012.—The goal of this study was to determine whether administration of the CB_1 cannabinoid receptor antagonist rimonabant would alter fatty acid flux in nonhuman primates. Five adult baboons (*Papio Sp*) aged 12.1 ± 4.7 yr (body weight: 31.9 ± 2.1 kg) underwent repeated metabolic tests to determine fatty acid and TG flux before and after 7 wk of treatment with rimonabant (15 mg/day). Animals were fed ad libitum diets, and stable isotopes were administered via diet (d_{31}-tripalmitin) and intravenously ($^{13}C_4$-palmitate, $^{13}C_1$-acetate). Plasma was collected in the fed and fasted states, and blood lipids were analyzed by GC-MS. DEXA was used to assess body composition and a hyperinsulinemic euglycemic clamp used to assess insulin-mediated glucose disposal. During the study, no changes were observed in food intake, body weight, plasma, and tissue endocannabinoid concentrations or the quantity of liver-TG fatty acids originating from de novo lipogenesis (19 ± 6 vs. 16 ± 5%, for pre- and posttreatment, respectively, $P = 0.39$). However, waist circumference was significantly reduced 4% in the treated animals ($P < 0.04$), glucose disposal increased 30% ($P = 0.03$), and FFA turnover increased 37% ($P = 0.02$). The faster FFA flux was consistent with a 43% reduction in these fatty acids used for TRL-TG synthesis (40 ± 3 vs. 23 ± 4%, $P = 0.02$) and a twofold increase in TRL-TG turnover (1.5 ± 0.9 vs. 3.1 ± 1.4 $\mu mol \cdot kg^{-1} \cdot h^{-1}$, $P = 0.03$). These data support the potential for a strong effect of CB_1 receptor antagonism at the level of adipose tissue, resulting in improvements in fasting turnover of fatty acids at the whole body level, central adipose storage, and significant improvements in glucose homeostasis.

endocannabinoid; adipose; fatty acid flux; stable isotopes; baboon

THE CB_1 CANNABINOID RECEPTOR (CB_1R) and its endogenous ligands, the endocannabinoids, have emerged as key players in the control of energy balance. Large-scale, randomized clinical trials of endocannabinoid antagonist treatment (e.g., rimonabant) in humans demonstrated significant improvements in cardiovascular risk factors, although psychiatric side effects caused the drug to be removed from the market (15). Despite this setback, and given the recognition that endocannabinoids (EC) interact with other systems (e.g., inflammation, insulin signaling), research in this area has remained extremely active, and peripherally restricted cannabinoid antagonist-based therapy may still have a place in the improvement of insulin sensitivity. A good deal of recent human research has focused on the tissue distribution, concentrations, and peripheral effects of the endocannabinoids 2-arachidonoyl glycerol (2-AG) and anandamide (AEA) and the fatty acid ethanolamides oleoylethanolamide (OEA) and palmitoylethanolamide (PEA). The levels of these molecules in plasma and tissue are related to obesity (5, 20), insulin resistance (11), and diabetes (25, 39). Cannabinoids are lipids that signal through fatty acid means, and a common theme emerging from the basic (25, 39), cellular, and animal research (31, 61) is that their influence on metabolism may be mediated through alterations in fatty acid balance. Early data from rodent studies demonstrated that treatment with an EC agonist elevated liver fatty acid synthesis (41) and that treatment of *ob/ob* mice with rimonabant reduced hepatic lipogenesis (42). In humans, obesity is associated separately with elevated plasma endocannabinoid concentrations (24) and increased hepatic de novo fatty acids (23, 54), and thus, whether rimonabant treatment would reduce fatty acid synthesis in an animal model with physiology more close to humans is unknown. Because treatment of human subjects with rimonabant produced weight loss, it has been difficult to separate the beneficial effects of EC antagonist treatment from the metabolic improvements occurring after weight reduction. No tests of fatty acid synthesis or flux have been performed in large animals or humans at weight stability, and metabolic studies available in the literature have often been complicated by changes in food intake and body weight. Therefore, the present investigation utilized repeated kinetic analysis to assess the treatment effect of the CB_1 antagonist rimonabant on lipid flux in the baboon (*Papio*) at weight stability. The close evolutionary relationship between humans and nonhuman primates suggests that they share many of the specific genetic mechanisms involved in determining differential susceptibility to disease (18). Not only do nonhuman primates offer a large, long-lived animal for the study of chronic diseases associated with metabolic dysregulation (13, 14, 27, 66), they provide a model that is genetically very similar to humans. The present study was designed to test whether the insulin-sensitizing

* These two authors contributed equally to this article.

Address for reprint requests and other correspondence: E. Parks, Center for Human Nutrition, Univ. of Texas Southwestern Medical Center, 5323 Harry Hines Blvd., Dallas, TX 75390-9052 (e-mail: Elizabeth.Parks@UTsouthwestern.edu).

effects of rimonabant would result in a significant reduction in de novo lipogenesis in the baboon and whether improvements in glucose metabolism would be coincident with improvements in adipose lipid flux. The dosage of rimonabant (15 mg/day) was set to not cause a change in food intake and body weight or produce characteristics of depression in the baboons. As described below, these findings have implications for the role of EC blockade to mediate improvements in metabolic dysfunction through the adipose and support the potential for modulation of the peripheral EC system in the development of future treatments for metabolic diseases.

METHODS

Animals and study design. The baboons studied herein were selected from a population at the Southwest National Primate Research Center located at the Texas Biomedical Research Institute (San Antonio, TX). The overall study design is shown in Fig. 1. From a larger group of animals (*Papio)*, five male baboons that were 7.5–18.1 yr of age (i.e., fully sexually mature) were chosen. Each animal was housed in an individual cage. Given the labor-intensive nature of these studies, animals were studied one at a time, sequentially, over a 3-yr period. The light cycle in the clinic room was set every day from 0600 to 1800. During an acclimation phase (Fig. 1), each animal was observed for aggressive/submissive behaviors, daily food consumption was monitored, and the animal was accustomed to the tether jacket system (16). After it was determined that the animal would acclimate to these surroundings it underwent ketamine sedation, and baseline assessments were made as follows: body composition by dual-energy X-ray absorptiometry scan (DEXA; Lunar Prodigy whole body scanner; GE Medical Systems, Madison, WI), measurements of body weight, waist circumference, and body surface area, and blood sampling for clinical biochemistries. A hyperinsulinemic euglycemic clamp study was performed the same day using previously published methods (13, 14). Following these assessments, the animal underwent surgical tether implantation, as described in detail previously (16). On the same day, biopsy samples of liver, subcutaneous adipose tissue (SubQ), and omentum, i.e., visceral adipose tissue (VAT), were taken. Tissue was frozen in liquid nitrogen immediately after biopsy.

During a 24-h period after catheter placement, the animal was carefully monitored. After a recuperation period of 2 wk, a stable isotope study was performed to quantitate fatty acid and TG flux, as described below. After the isotope study, the animal began treatment with rimonabant (15 mg/day, full-form qd in the morning) mixed in a peanut butter-based sweet treat for 7 wk. The dose of rimonabant chosen was based on a pharmacokinetic study performed earlier and chosen to limit weight loss and side effects. At the end of the treatment phase, metabolic study procedures were repeated. Following these studies the tether and catheters were removed surgically under isoflurane, and the animal was monitored again until it recuperated. All study interventions and animal experiments were conducted according to the protocols approved by the Institutional Animal Care and Use Committee of the Texas Biomedical Research Institute. All animals received humane care according to the criteria outlined in the *Guide for the Care and Use of Laboratory Animals* prepared by the National Academy of Sciences and published by the National Institutes of Health (NIH publication no. 86-23, revised 1985).

Dietary intake and isotope-labeling scheme. For all animals, food was made available throughout the study from 0800 to 1600 each day, and animals were acclimatized to this feeding time. This protocol was used to obtain a definitive time when animals would have been actively eating (0800–1300) to investigate postprandial metabolism. Food intake and changes in behavior (e.g., depressive posture, interactions with handlers) were monitored daily by technical staff. As described in detail elsewhere (4), the standard diet (Monkey Diet 15%, Constant Nutrition Purina 5LE0) contained 57.7% carbohydrate (g/100 g weight), 15.3% protein, and 4.7% fat (ether extract). The animals were offered a quantity of food daily that was based on the estimated metabolizable energy requirements for adult captive baboons (39a) and designed to meet an expected energy requirement to sustain constant body weight (40–51 kcal/body wt in kg). This quantity of energy was adjusted based on the weekly measurements of the animal such that food was provided just in excess of that needed to maintain weight. Water was provided to the animals ad libitum, and fresh fruits and vegetables were given for enrichment. Immediately before receiving their food each morning, animals received a single peanut butter sweet treat, which contained the dose of rimonabant. Only on the day of the isotope study was the drug also combined with glyceryl-d_{31}-tripalmitin, which allowed for identification of dietary fatty acids in the blood of the animals. The dietary label and the intravenous (iv) isotope studies were performed by modifying human protocols used previously while taking into account the different metabolic body size of the baboon (4, 33, 62, 63). At 0800 on the day of the isotope infusion study, an iv infusion of [$^{13}C_1$]sodium acetate (5 g dissolved in ½ normal saline, infusion rate of 1.0 ml/min) was begun to achieve labeling of fatty acids made through the de novo lipogenesis pathway. This infusion continued for 23 h. Metabolite and hormone data from the fasting state represent analysis of blood taken before 0800. Blood was drawn at 1100, 1200, and 1300 in the postprandial state, and data presented in Table 1 for the fed state represented the average of these three values. At 1600, the food was removed as per daily protocol. To reduce stress, fasting metabolism in the baboons was assessed at night and under light sedation, as

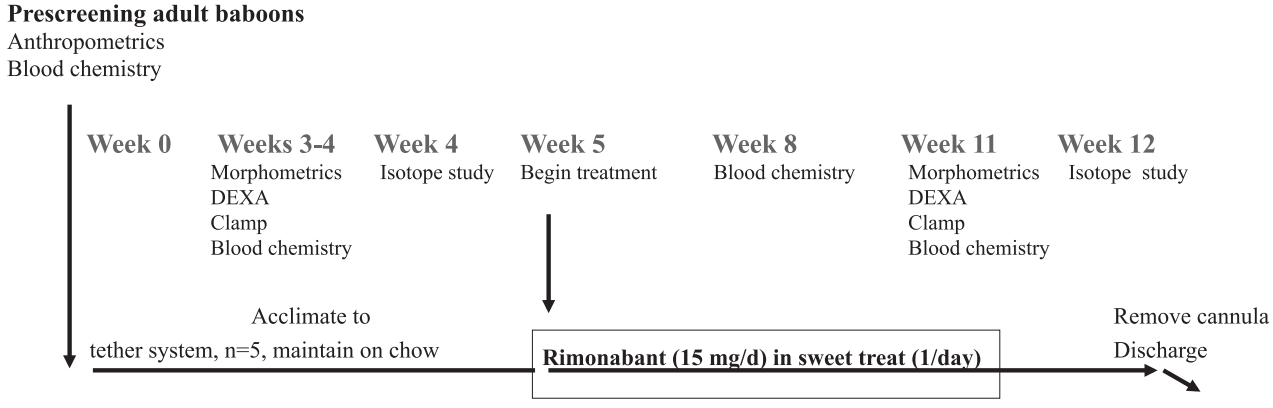

Fig. 1. Study timeline. Five male baboons were studied over a 12-wk period to determine the effect of 15 mg·kg^{-1}·day^{-1} of the cannibinoid (CB_1) antagonist rimonabant. For details of procedures, see METHODS. DEXA, dual-energy X-ray absorptiometry.

Table 1. *Animal characteristics*

Variable (Anthropometrics)*	Time Points		*P* Value
	Baseline	7 Wk	
Body weight, kg	31.6 ± 1.1	31.2 ± 1.6	0.141
Body fat mass, kg	2.7 ± 0.6	2.5 ± 0.6	0.302
%Body fat mass	8.7 ± 1.8	7.8 ± 1.6	0.256
Lean mass, kg	27.7 ± 0.5	27.4 ± 0.5	0.293
%Lean mass	88.4 ± 1.6	89.6 ± 0.9	0.486
Waist circumference, cm	59.0 ± 1.1	56.5 ± 1.9	0.039
Trunk fat, kg	1.59 ± 0.56	1.12 ± 0.30	0.257
TRL-TG, mmol/l	0.11 ± 0.03	0.12 ± 0.06	0.372
TRL-B48, ng/ml	118 ± 47	114 ± 13	0.472
Insulin, μU/ml	7.9 ± 3.4	6.2 ± 2.3	0.298
Glucose, mmol/l	4.8 ± 0.2	5.0 ± 0.2	0.195
FFA, mmol/l	0.45 ± 0.09	0.37 ± 0.07	0.170
Ketone bodies, μmol/l	94 ± 26	89 ± 16	0.312

Values are means ± SE. TRL, triacylglycerol-rich lipoproteins; TG, triacylglycerol; B48, apolipoprotein B48; FFA, free fatty acids. *Treatment group; $n = 5$ male baboons. Paired *t*-tests were used to test for significant differences. Plasma TG and TRL-TG values were log transformed before analysis. Values are of fasting metabolites derived from the first blood draw on the morning of the isotope infusion study.

described previously (4). Accordingly, at 1900, a 0.025 mg/kg bolus dose of midazolam was given, followed by midazolam infusion (0.04 $mg \cdot kg^{-1} \cdot h^{-1}$) to calm the animal. This light sedation was continued until the end of the isotope study on *day 2* at 0700, and the animals rested or slept when the measurements were made. At 2255, an iv infusion of isotopes that contained [d_5]glycerol (5 mg·kg lean body $mass^{-1} \cdot h^{-1}$) and K^+[1,2,3,4-$^{13}C_4$]palmitate (7 $\mu g \cdot kg^{-1} \cdot min^{-1}$) complexed to human albumin in a ratio of 2:1 was begun. During the night, blood was drawn at 2300, 2320, 2340, 2400, 0030, 0100, 0130, 0200, 0300, 0430, 0600, and 0700. All isotopes and the midazolam were infused through a catheter into the femoral vein, and the blood was drawn from the femoral artery through a different tethered catheter (4). Isotopes were purchased from Isotec (Miamisburg, OH) and from Cambridge Isotope Laboratory (Andover, MA), were sterile and pyrogen free, and were prepared using sterile techniques. Isotopic purity was >98% for all of the tracers used.

Analysis of metabolites, hormones, endocannabinoids, and rimonabant. Triacylglycerol (TG)-rich lipoproteins (TRL) consisting of chylomicrons and VLDL ($d < 1.006$ g/l) in the fed and fasted states were isolated from plasma by ultracentrifugation, as described previously (4). For measurements of plasma-TG, TRL-TG, glucose, and free fatty acid (FFA) concentrations, enzymatic kits were used (nos. 461-09092, 461-08992, 439-90901, 999-34691, and 991-34891, respectively; WAKO, Richmond, VA). TRL-B48 concentration was measured using a human apoB-48 ELISA kit (Shibayagi), and insulin was measured by Millipore ELISA kit for human insulin (no. EZHI-14K). Systemic rimonabant concentrations in plasma were measured by Sanofi researchers. Briefly, samples from baseline, 3.5 wk, and 7 wk were mixed with 50 μl of internal standard solution (25.0 ng/ml of SR141716-D10 in acetonitrile). The tubes were vortexed and centrifuged at 10,000 *g* for 5 min. An aliquot of the supernatant (50 μl) was transferred into an autosampler vial and mixed with 100 μl of water for LC-MS-MS analysis. The lower limit of quantitation for SR141716 and its primary metabolite SR141715 in samples was 0.25 ng/ml. The endocannabinoids AEA and 2-AG and the anandamide-like fatty acid ethanolamides OEA and PEA were measured in plasma and in SubQ and VAT biopsy samples by HPLC-MS, as described previously (26, 22). Plasma EC concentrations were measured at baseline, 3.5 wk, and 7 wk, whereas tissue concentrations were measured in biopsy samples taken at baseline and 7 wk. Liver biopsy samples were used to measure liver-TG content, as described previously (32).

Analysis of fatty acid composition and fatty acid and glycerol turnover. The fatty acid compositions of TRL-TG fatty acids and plasma FFA were analyzed on a HP 6890 series gas chromatograph, as described previously (4). To determine isotopic enrichments, the GC-MS method utilized selected ion monitoring for mass-to-charge ratios (*m/z*) of 270, 271, 272, 274, 300, and 301. Palmitate methyl ester enrichments were calculated using five-point standard curves for M_4 and (d_{30} + d_{31}) analysis. The measurement of newly made fatty acids was performed with *m/z* of 270, 271, and 272 and calculated using the mass isotopomer distribution analysis method (28). Isotopomers of the propionic ester of glycerol (*m/z* 171, 172, 173, 175, and 176) were assessed in the electron impact mode, as described by Sunehag et al. (60). The fragment assessed for the derivatized d_5-glycerol had a *m/z* of 173, and the 175/176 ions were derived from the internal standard that was added ($^{13}C_3$, d_8-glycerol). Comparable ion peak areas between the standard curve and biological samples were achieved by either diluting or concentrating the sample.

Calculations and statistical analysis. The fatty acid infusate compositions and enrichments were analyzed by GC and GC-MS, as described previously (4). In the present analysis, palmitate is used as the fatty acid marker for all fatty acids in TG (i.e., the contribution of plasma palmitate in the FFA pool is assumed to contribute to liver-TG synthesis as efficiently as other fatty acids in the FFA pool). The contribution of dietary fatty acids to the plasma FFA pool was determined as follows: %FFA from dietary spillover:

$$\frac{\left[\text{fraction of } d_{31}\text{-palmitate in FFA}\right]}{\left[\text{fraction of } d_{31}\text{-palmitate in the sweet treat-TG}\right]}$$

Fasting lipolysis was assessed by measuring the rate of appearance of plasma FFA (R_a FFA) and of plasma free glycerol (R_a glycerol) during the night. The final R_a FFA and R_a glycerol data for a single baboon were determined from steady-state values collected between 0300 and 0700 (from 4–8 h after the start of the infusion). The measurement of TRL-TG turnover, in units of $\mu mol \cdot kg^{-1} \cdot h^{-1}$, represents the production of lipoprotein-TG from the liver and the clearance of TG from the blood. This turnover was calculated by modeling the rise to plateau of the plasma FFA label (M_4-palmitate enrichment) in TG over the time frame of 2400 to 0700. To test for changes in TRL-TG assembly in the liver, the variously labeled methyl palmitate isotopomers in TG were analyzed as the proportion of total methyl palmitate found in TG (2). The values used to obtain these fasted sources were derived from the average contributions of sources in TRL-TG from samples collected between 0400 and 0700. Thus, the contributions of various sources (dietary fat, plasma FFA derived from adipose tissue, and fatty acids made via de novo lipogenesis) of TRL-TG fatty acid are presented here as a proportion, which reflects the fluxes of fatty acids into the intrahepatic TG synthesis machinery (VLDL-TG synthetic processes). The proportions of palmitate derived from the sources were then multiplied by the absolute concentration of TRL-TG fatty acids to determine their quantitative contributions of these sources to blood-TG concentrations. It is possible that not all fatty acid sources will be identified using this scheme, as we have demonstrated previously (23, 45). The fatty acids that remain unlabeled at the end of the 23-h study could be derived from visceral stores or from intrahepatic-TG droplets. Calculations were performed using Excel (version 2007; Microsoft, Seattle, WA), and statistical analysis was conducted using Statview for Windows (Version 5.0.1; SAS Institute, Berkeley, CA). Data were tested for skewness and log-transformed when parametric analysis assumptions were not met. For paired *t*-tests, statistical significance was taken as a *P* value of ≤0.05. Repeated-measures ANOVA was used to test baseline, 3.5-wk, and 7-wk concentrations of plasma rimonabant concentrations, with a *P* value of 0.05 to denote significance. The association between outcome variables was assessed with Pearson's correlation coefficients. Simple linear regression was performed using a layered Bonferroni correction for multiple comparisons.

RESULTS

Morphometric and biochemical changes, concentrations of rimonabant, and EC. Food intake was monitored daily for each animal and was unaffected by rimonabant treatment (data not shown), nor was treatment associated with changes in baboon body weight, body fat, or lean mass (Table 1). Waist circumference was reduced 4% starting from 59.0 ± 1.1 cm at baseline, achieving 57.1 ± 0.8 cm at the midpoint of the study (3.5 wk; data not shown), and ending at 56.5 ± 1.9 cm at 7 wk ($P = 0.039$; Table 1). No changes in fasting concentrations of plasma lipids, FFA, ketone bodies, glucose, or insulin were observed. Figure 2*A* displays the concentrations of rimonabant (SR141716) and its primary metabolite (SR141715) in plasma, which verifies that the sweet treat containing the compound was a sufficient vehicle for daily drug delivery. Concentrations of both compounds were elevated significantly above the respective baseline levels by 3.5 wk, and the 3.5- and 7-wk concentrations were not different from one another (Fig. 2*A*). The interanimal variability of concentrations of the metabolite SR141715 was low compared with the variability of plasma rimonabant between animals. Steady-state concentrations were reached for the metabolite, which suggested that the capacity for rimonabant metabolism had been maximized. The apparent continued rise of plasma rimonabant concentrations between 3.5 and 7 wk supported the concept of recycling of the compound out of tissues, which would have reached a maximum at 100 days. Indeed, plasma rimonabant concentration at 3.5 wk was associated significantly with total body weight ($r = 0.940$, $P = 0.05$), but no significant relationships were detected between plasma rimonabant concentration and any measurement of body composition at 7 wk.

Concentrations of the endocannabinoids AEA and 2-AG and the anandamide-like non-CB_1 receptor-binding fatty acid ethanolamides OEA and PEA were measured in plasma and in SubQ and VAT (omental) biopsy samples (baseline and 7 wk). To our knowledge, in nonhuman primates, plasma and tissue EC concentrations have not been published before. At baseline, fasting plasma AEA concentrations (2.2 ± 1.3 pmol/ml) were similar to those reported previously in humans (10, 24, 65), as were 2-AG concentrations (45.3 ± 34.6 pmol/ml) (65). At baseline, plasma concentrations of OEA were 16.0 ± 8.7 pmol/ml and PEA 3.7 ± 0.8 pmol/ml. Within adipose depot types, OEA concentration was significantly higher in VAT (81.0 ± 62.2 pmol/g) compared with SubQ (38.2 ± 41.8 pmol/g, $P = 0.05$). At 7 wk, the higher the SubQ concentrations of OEA and PEA, the greater the animal's body fat

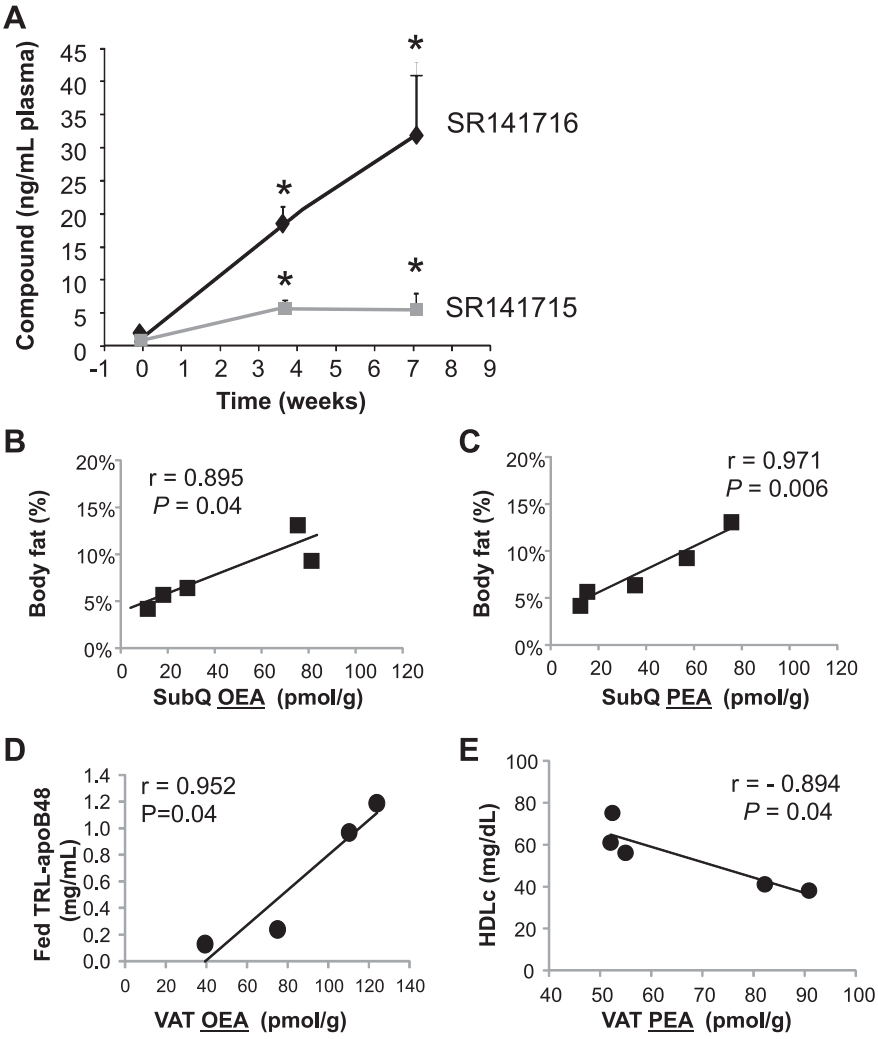

Fig. 2. Plasma concentrations of rimonabant and its primary metabolite and the association between subcutaneous oleoylethanolamide (OEA) and palmitoylethanolamide (PEA) and body fat. Values are means ± SE. *A*: plasma concentrations of rimonabant (SR141716) and its primary metabolite (SR141715) at baseline, 3.5 wk, and 7 wk posttreatment in 4 baboons. For both the drug and its metabolite, concentrations at 3.5 and 7 wk were significantly greater (*$P < 0.05$) than their respective concentrations at baseline (i.e., before drug treatment). *B* and *C*: relationships were explored between 7-wk concentrations of subcutaneous adipose tissue (SubQ) OEA (*B*) and PEA (*C*) and %body fat content. *D* and *E*: at 7 wk, higher visceral adipose tissue (VAT) OEA (*D*) and PEA (*E*) concentrations were associated with greater triacylglycerol (TG)-rich lipoprotein (TRL)-apolipoprotein B48 lower and HDL cholesterol, respectively.

percentage (Fig. 2, *B* and *C*) and waist circumference (data not shown), whereas the higher the VAT OEA, the greater the fed TRL-apoB48 concentration (Fig. 2*D*), and the higher the VAT PEA, the lower the fasting HDL cholesterol concentrations (Fig. 2*E*).

Glucose disposal, TRL-TG turnover, and kinetic measures of lipolysis. Treatment with rimonabant for 7 wk did not change fasting glucose concentrations (Table 1). However, measurement of glucose disposal rates by the hyperinsulinemic euglycemic clamp showed a significant 31% increase posttreatment ($P = 0.033$; Fig. 3*A*). Furthermore, the turnover of plasma TG carried in the TRLs increased twofold ($P = 0.033$; Fig. 3*B*). Using continuous infusion of both [d_5]glycerol and [$^{13}C_4$]palmitate, fasting adipose lipolysis rates were measured from midnight to 0700. Although no change in plasma glycerol turnover was observed posttreatment (R_a Glycerol; Fig. 3*C*), the R_a FFA from adipose was 37% higher ($P = 0.024$; Fig. 3*D*). The higher ratio of the FFA and glycerol fluxes suggests that intra-adipocyte fatty acid reesterification was suppressed by treatment (34). The concentrations of plasma AEA at baseline were positively associated with fasting insulin concentrations ($r = 0.960$, $P = 0.01$;Fig. 3*E*), whereas at 7 wk, plasma AEA concentrations were negatively associated with glucose disposal ($r = -0.898$, $P = 0.03$; Fig. 3*F*).

Sources of plasma FFA. Plasma FFA can be derived from adipose tissue release or from TG lipolysis intravascularly. The contributions of these sources to total plasma FFA concentrations over time were identified utilizing the isotopic labeling scheme before and after treatment. At baseline (Fig. 4*A*, *left*), total plasma FFA concentrations rose after the onset of eating (Fig. 4*A*, open circles between 1000 and 1300) as a result of both a small increase in adipose fatty acids (Fig. 4*A*, open triangles) and a large contribution of dietary fatty acids (Fig. 4*A*, gray squares). During the night (between 2200 and 0200), total FFA concentrations were surprisingly high and did not return to fasting levels until 0430. Food was removed from the animal's cage at 1600, yet residual dietary fatty acids were present in the plasma FFA pool throughout the night (Fig. 4*A*,

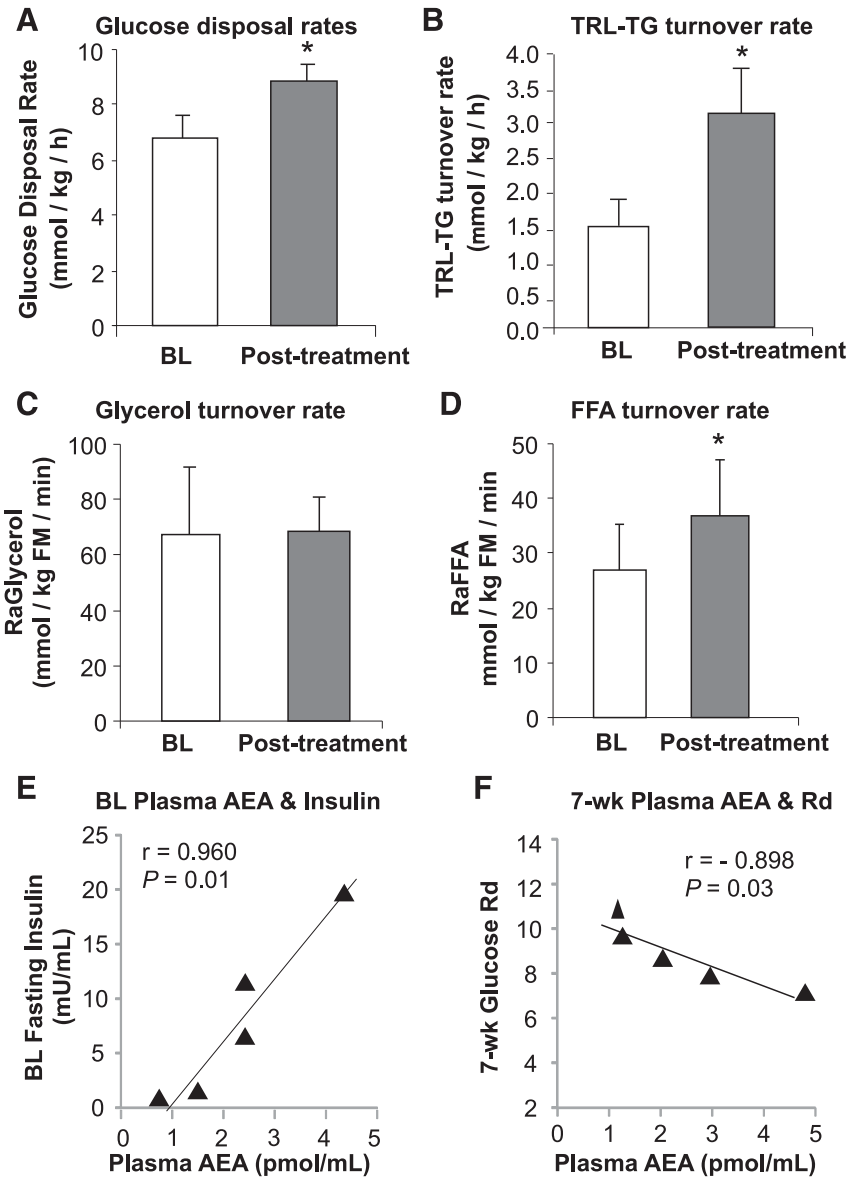

Fig. 3. Changes in metabolic variables over time. *A–D*: changes in glucose disposal rates (*A*), TRL-TG turnover (*B*), rate of appearance of plasma glycerol (R_a Glycerol; *C*), and rate of appearance of of free fatty acids (R_a FFA; *D*) ($n = 5$). *Significant differences from the corresponding baseline (BL) time points. Relationships were explored between BL fasting plasma anandamide (AEA) concentrations and fasting plasma insulin (*E*) and posttreatment AEA and glucose disposal rates (R_d) (*F*).

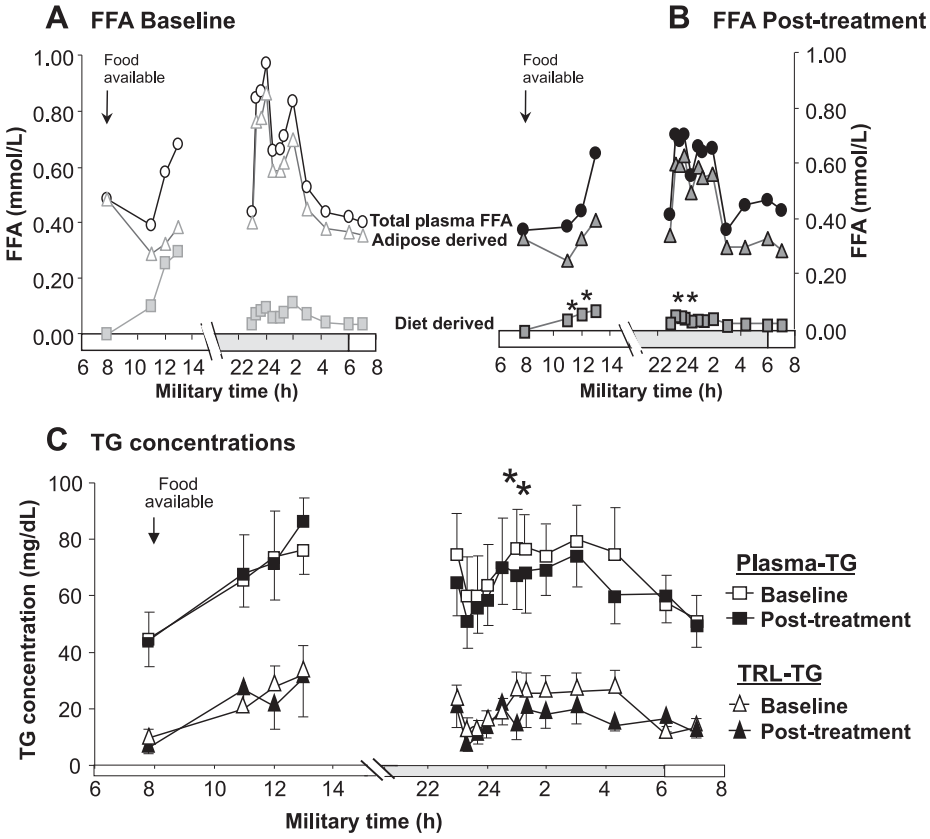

Fig. 4. Sources of plasma FFA and concentrations of plasma TG and TRL-TG. *A* and *B*: total concentrations and sources of plasma FFA ($n = 5$) over 23 h at BL (*A*) and posttreatment (*B*), with error bars removed for visual clarity. Circles, total plasma FFA concentrations; triangles, plasma FFA derived from adipose release; squares, plasma FFA derived from dietary TG-fatty acids. *C*: concentrations of total plasma TG (*top data*, □ and ■) and TRL-TG (*bottom data*, △ and ▲) over 24 h at BL (△ and □) and posttreatment (▲ and ■). Food was made available to the animals from 0800 to 1600 each day. *Significant differences from the corresponding BL time points.

gray squares). This could have resulted from either nocturnal release of chylomicrons labeled the previous day (11) or recycling of a previously stored label. After treatment with rimonabant (Fig. 4*A*, *right*), total plasma FFA concentrations again rose postprandially between 1000 and 1300 in a pattern similar to that observed at baseline. However, compared with pretreatment, significantly fewer dietary fatty acids were found in FFA between 1000 and 1300 posttreatment. During the night, diet-derived fatty acids were also lower compared with baseline.

TG concentrations and fatty acid sources used for TG synthesis. As shown in Fig. 4*C*, total plasma TG concentrations were unchanged by treatment during the fed state (open vs. closed squares), but during the night, plasma TG concentrations were lower posttreatment compared with baseline. A similar treatment-related reduction for the nighttime TRL-TG concentrations was also observed, but the changes did not reach statistical significance (Fig. 4*C*, closed triangles). When the change in nighttime concentrations of plasma TG was calculated, those animals with the greatest absolute reductions in TG concentrations had the highest rimonabant concentrations in blood ($r = 0.996$, $P < 0.02$). The changes in the nighttime plasma TG concentrations were due to an increased uptake of the lipids since treatment increased TRL-TG turnover rate significantly (Fig. 3*B*).

The sources of fatty acids used to synthesize TRL-TG, made up primarily of hepatically derived VLDL during the night, were identified using stable isotope labeling of adipose FFA release, fatty acids made through the de novo lipogenesis pathway in the liver, and fatty acids originating from dietary TG. Figure 5*A* presents the analysis of these sources and demonstrates that, at baseline, of all the fatty acids found in TG, the sources of 75.9 ± 3.3% of them were identified using the labeling scheme. Of this proportion, dietary sources made up the smallest percentage (16.2 ± 4.1%), with slightly more coming from de novo lipogenesis and the majority originating from the plasma FFA pool (40.4 ± 2.5%). Posttreatment, a smaller proportion of TG fatty acids became labeled (49.5 ± 7.1%, $P = 0.008$ compared with baseline). The relative amounts of dietary and de novo fatty acid represented similar proportions as found at baseline (Fig. 5*A*). However, the proportion of TG fatty acids derived from the plasma FFA pool fell to 57% of the baseline level ($P = 0.009$).

Finally, the proportions of TG fatty acids derived from the sources were multiplied by the total quantity of fasting TRL-TG fatty acids in the blood for each animal to obtain the absolute contributions of these sources to blood TG (Fig. 5*B*). Fasting TRL-TG fatty acid concentrations were not different between baseline and posttreatment (0.90 ± 0.23 and 0.77 ± 0.17 mmol/l, respectively, $P = 0.214$), but the absolute amounts of fatty acids identified by labeling were 26% lower after treatment ($P = 0.01$). Of that labeled, the amounts of fatty acids derived from the diet and from de novo lipogenesis were not different after treatment, but the quantity of TRL-TG made from the plasma FFA pool was 46% lower (0.35 ± 0.08 vs. 0.19 ± 0.06 mmol/l for baseline and posttreatment, respectively, $P = 0.02$). After rimonabant, the sources of more TRL-TG fatty acids remained unidentified at the end of the study ($P = 0.01$). As described above, these fatty acids could have come to the liver through visceral TG depot release or could have been derived from TG stores within the liver. Indeed, analysis of liver TG contents from biopsy samples

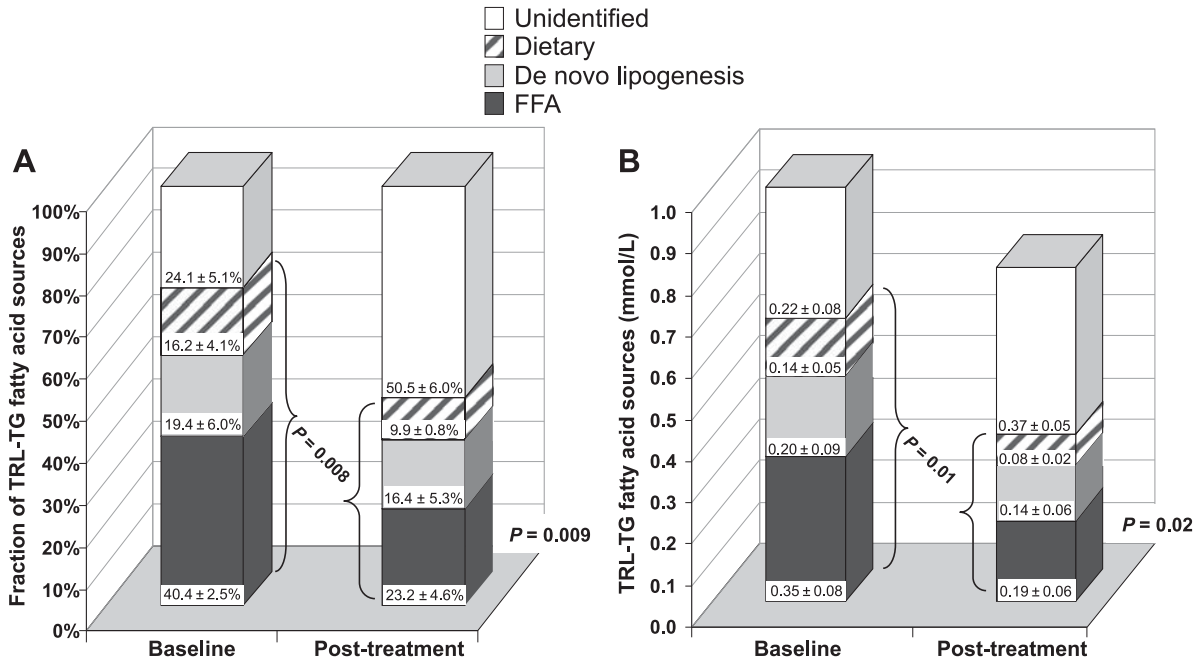

Fig. 5. Fractional and absolute quantity of TRL-TG fatty acid sources identified by isotopic labeling. Data represent the contribution of TRL-TG fatty acids derived from the adipose, via the plasma FFA pool (dark gray bars at the base of the column), from carbohydrates via hepatic de novo lipogenesis (light gray bars), from dietary TG (hatched bars), and for fatty acids not labeled (source unidentified) during the course of the 23-h experiment (open bars). The sources of fatty acids are presented as they contributed proportionally to TRL-TG synthesis (*A*) and to the absolute synthesis of TRL-TG (*B*). The total amount of fatty acid sources accounted for using the isotopic labeling scheme were found to be different whether the data were considered in units of percent ($P = 0.008$) or mmol/l ($P = 0.01$).

demonstrated an increase in liver stores after treatment (20 ± 2 vs. 35 ± 8 nmol/mg protein at baseline and posttreatment, respectively, $P = 0.046$). Plasma rimonabant concentrations did not correlate with the presence of de novo lipogenesis fatty acids when tested either as a percentage of total TRL-TG or as the absolute quantity derived from lipogenesis. The reduction in TG derived from plasma FFA was negatively correlated with the plasma rimonabant concentration ($r = -0.998$, $P = 0.002$); i.e., the higher the plasma rimonabant concentration, the greater the reduction in the use of these plasma FFA for lipoprotein TG synthesis in the liver.

DISCUSSION

The present investigation utilized kinetic analysis to assess the treatment effect of the CB_1 receptor antagonist rimonabant on lipid flux in weight stable, nonhuman primates. Our hypotheses were that *1*) the insulin-sensitizing effects of the drug would reduce lipogenesis in the nonhuman primate *Papio*, as has been demonstrated in mice (19, 41, 42); and *2*) improvements in glucose metabolism would be coincident with improvements in adipose lipid flux, as implicated previously in rodent studies (49) and in cell culture (6, 43). After completion of 7 wk of treatment, rimonabant did not reduce hepatic de novo lipogenesis, which was a surprise. Rather, in the absence of weight loss we observed significant improvements in glucose metabolism, greater whole body turnover, disposal of fatty acids and TG, and a significant metabolic impact of the drug evident during the night, which included more efficient disposal of dietary fatty acids consumed the previous day. As described below, these findings have implications for the role of CB_1 receptor blockade to mediate improvements in metabolic dysfunction through the adipose and support the potential for modulation of the peripheral EC system in the development of future treatments for metabolic diseases.

In the baboon studies here, although rimonabant treatment did not change EC concentrations in plasma or adipose tissues, treatment uncovered significant relationships between the EC and lipid-related variables, similar to relationships observed previously in humans (21). At baseline, plasma AEA concentrations were elevated in those animals with higher fasting insulin concentrations, whereas after treatment, higher AEA concentrations were associated with lower glucose disposal rates ($P < 0.05$). Furthermore, posttreatment, higher concentrations of SubQ and VAT OEA and PEA were tightly associated ($r > 0.75$) with greater amounts of adipose mass, a finding similar to those of Guardado-Mendoza et al. (27), Horeau et al. (30), and Matias et al. (37), who showed that PEA is the ethanolamide secreted in the highest concentration from human primary adipocytes in culture. In line with the ethanolamides' role in metabolic dysfunction, baboon VAT OEA and PEA concentrations were associated with higher fed-state concentrations of intestinal lipoproteins in plasma (apoB48 concentrations) and lower HDL cholesterol concentrations (Fig. 2*E*). That these associations were present only after 7 wk (and not at baselines) is likely due to the uniformity of the conditions of housing in the clinic (same feeding time for all of the animals, common diet, reduced physical activity, etc.). These observations support a negative influence of the cannabinoid system on lipid metabolism and underscore the similarities of the EC/insulin sensitivity axis between baboons and humans (21).

The first of our hypotheses was that hepatic lipogenesis would be reduced significantly after rimonabant treatment,

even at weight stability. This hypothesis was based on much data from rodent studies demonstrating that treatment with an EC agonist elevated liver fatty acid synthesis (41), that the liver CB_1 receptor in mice is required for stimulation of fatty acid synthesis during high-fat feeding, and that treatment of *ob/ob* mice with rimonabant reduced hepatic lipogenesis (42). In humans, obesity is separately associated with elevated plasma EC concentrations (24) and increased hepatic de novo fatty acids, as evidenced by analysis of liver TG directly (23, 48) and of VLDL-TG, a validated marker of hepatic lipogenesis (23, 54). Analyzing the presence of newly made fatty acids in VLDL-TG before and after treatment, we found no significant differences. Our lack of ability to detect a change in lipogenesis was not due to low basal levels of fatty acid synthesis. Compared with humans in which fasting lipogenesis contributes 0–12% of VLDL-TG palmitate, baboons exhibited higher levels (19%), presumably because of the higher content of carbohydrate in their diet (69% of total dietary energy). The lack of treatment-induced changes in lipogenesis observed here suggests that the role of the EC system to increase lipogenesis in rodents and the beneficial effect of rimonabant to reduce lipogenesis are dependent on alterations in food intake. It is well established that lipogenesis is a process exquisitely sensitive to negative energy balance (28, 55).

The second key finding of the present study was a rimonabant-induced improvement in macronutrient metabolism at multiple physiological levels. Blüher et al. (10) showed that high plasma 2-AG concentrations correlated negatively with glucose disposal rates in humans, as we have found here in baboons (Fig. 3*F*). Furthermore, the 30% improvement in glucose disposal rates during the clamp echoes significant reductions in 2-h glucose post-oral glucose tolerance test found in humans, although the latter occurred against a backdrop of body weight loss (39b). From a lipid metabolism perspective, a 37% increase in plasma FFA turnover was observed after treatment (Fig. 3*D*), which is consistent with a growing body of research. Evidence of a role for EC to modulate adipose tissue metabolism includes the discovery of cannabinoid receptors CB_1R and CB_2R in human omental and SubQ adipocytes (51), increased glucose uptake into adipocytes and lipid droplet formation following CB_1R stimulation (36), and abrogation of the latter effect by CB_1R antagonism in primary human adipocytes (43). In the baboons, the combined turnover data from both plasma glycerol and FFA suggested that rimonabant reduced adipose reesterification rates, resulting in greater outflow of FFA from adipose. Furthermore, the baboon's waist circumferences became significantly reduced with treatment. Redistribution of body fat in the absence of loss of total body weight has been observed before with other insulin sensitizers such as pioglitazone (38, 57). Although rimonabant-induced weight loss in humans has resulted in reductions in waist circumference (15), the observations here were completely unanticipated due to the constancy of the animals' body weights. On the other hand, in accord with our findings, Richey et al. reported that 16 wk of rimonabant treatment in high-fat fed dogs reduced subcutaneous adipose tissue accumulation by 20% and also prevented a diet-induced expansion of visceral adipose fat (50).

The present kinetic data suggest that the reductions in adipose accumulation in mice and dogs observed previously were due to a stimulation of fatty acid release from adipose as a result of lower reesterification intracellularly. Whether the impact of rimonabant on adipose metabolism is direct in primates and/or humans remains an open question (64). Early data from treated mice suggested that peripheral modulation by CB_1R antagonism was not a major mechanism for anti-obesity effects (46, 47, 59, 56). However, in addition to the research cited above, numerous recent studies from primary cell culture (25, 39) and tissue expression analysis (43, 51) provide evidence that CB_1R antagonists can exert their effects directly through adipocyte signaling (35), as reviewed elsewhere (44). Compared with central administration, intraperitoneal administration of rimonabant in rats led to independent effects of lipid mobilization in white adipose tissue (40), and Osei-Hyiaman et al. (42) have clearly shown that, in mice, hepatic-specific deletion of the CB_1R protects against diet-induced steatosis. Hence, one limitation of the present study is that it cannot be definitively determined whether the beneficial effects of treatment to change adipose metabolism were direct or mediated centrally. A test of the true direct effect of endocannabinoid antagonists on peripheral metabolism in vivo will await the development of compounds that do not cross the blood-brain barrier. Of note, the main limitations of this study are the small sample size that characterizes primate studies, a lack of control group, and the requisite isolation of the animals outside their typical social structure (required for the metabolic studies). These characteristics of the study design raise the issue of whether clinic housing alone would change any of these measures. Observations from animals kept in similar housing conditions suggest some variability in waist circumference over time and that metabolic markers such as insulin and FFA may worsen due to stress (Parks EJ and Bastarrachea RA, unpublished observations); if the latter two observations are reproducible, the present findings would be even more significant. Other study limitations include the measurement of whole body adipose tissue fatty acid release rather than depot-specific fatty acid release in vivo and a lack of direct measurement of visceral TG stores. Nonetheless, given the intensive nature of tracer studies, particularly in primates, the present results contribute important new findings of a dominant influence of the drug on adipose fatty acid and plasma TG turnover.

The third finding of this study was a significant increase in the plasma turnover of TG-rich lipoprotein particles in treated baboons. In humans, high plasma 2-AG concentrations correlated positively with serum TG concentrations (10), and SubQ levels of AEA, OEA, and PEA correlated negatively with SubQ lipoprotein lipase activity (1), which would serve to reduce TG clearance from plasma. In mice, chemically induced elevations in endogenously produced EC slow TG clearance, an effect that was absent in CB_1 knockout mice (53). In the treated baboons, the faster TG turnover equated to greater clearance of lipid from plasma and was also substantiated by a reduced presence of dietary fatty acids in the plasma FFA pool both postprandially and in the middle of the night (Fig. 4, *A* and *B*). Such spillover of chylomicron-derived fatty acids occurs when lipoprotein lipase activity outpaces tissue uptake (3). The significant relationship observed between VAT EC and fasting and fed TRL-B48 concentrations highlights recent discoveries regarding the role of EC metabolism and intestinal lipid absorption (22). Whether EC antagonism impacts intestinal lipid absorption and clearance via endocrine and/or paracrine effects will be important to determine. The significant positive rela-

tionships observed between body fat and SubQ levels of OEA and PEA (Fig. 2, *B* and *C*) suggest that the ethanolamides, being fat derived, may provide a global signal of elevations in fat storage. Since increased body fat is associated with enhanced inflammation, the increased levels of the potent anti-inflammatory PEA (30) may be evidence of a counter-regulatory response that is proportional to body fat content. Collectively, these data provide a metabolic connection to systematically link the mounting basic evidence of the control of the EC system on adipocyte (29), skeletal muscle (58), and intestinal biology (22) to impair lipid metabolism. Recent reports have also described the presence of both cannabinoid CB1 and CB2 receptors in rat pancreatic β-cells (7, 9) and in isolated human islets (8), adding the endocrine pancreas as a potential site in the regulation of glucose homeostasis and indicating a functional a role for endogenous endocannabinoid signaling in regulation of endocrine secretion in the pancreas. These data extend the strong congruence of evidence from various animal models supporting a principal role of the EC system to improve insulin sensitivity through mechanisms of lipid flux.

The fourth finding of this study involves the effect of rimonabant to lower the proportion of VLDL-TG fatty acids becoming labeled during the 23 h of stable isotope administration (Fig. 5). We have shown previously that the contribution of fatty acid sources used for synthesis of plasma VLDL-TG mirrors the contributions made to liver-TG pools assessed by biopsy (23). Thus, the increase in the "unlabeled fatty acid pool" seen in VLDL-TG posttreatment would suggest that the particles were assembled using either greater proportions of stored (cold) liver TG or fatty acids derived from visceral TG stores that were released to the liver. We speculate that both mechanisms may have been in play since, although liver TG increased significantly, it did not rise to levels of fatty liver, whereas the animal's waist circumferences became significantly (4%) reduced posttreatment. A number of other independent observations also support this concept and include faster FFA turnover (Fig. 3*D*), the lower proportional and absolute lipoprotein TG fatty acids labeled with the plasma FFA isotope, indicating that liver synthesis of VLDL-TG used almost half as many plasma FFA (Fig. 5, *A* and *B*), lower dietary spillover of chylomicron fatty acids (fig. 4, *A* and *B*), and no change in (or potentially even lower) plasma FFA concentrations, which combined provide evidence of greater clearance of FFA peripherally to organs other than liver (e.g., muscle and heart). The mechanism(s) by which rimonabant could improve fatty acid clearance peripherally is presently unknown but could include an increase in energy expenditure (12, 29).

In summary, the present study is the first to demonstrate in weight-stable animals the dominant effect of improved fatty acid kinetics as a result of treatment with an EC antagonist. Data from body composition, morphometrics, multiple isotope kinetics, and measurement of plasma and tissue cannabinoids provide direct evidence to support the hypothesis that antagonism of cannabinoid receptor signaling controls fat storage by regulating lipolysis and that improvement in fatty acid and TG disposal in the fasted and fed states provides the metabolic means to improve insulin sensitivity. It is unknown whether these changes were due to a direct effect of rimonabant on adipose tissue, an indirect effect orchestrated through neural circuits, or a combination of both of these mechanisms. However, the improvements in metabolic health in the absence of weight loss suggest that the development of new antagonists that do not cross the blood-brain barrier has potential as a future treatment for insulin resistance and diabetes. Finally, the significant relationships between plasma/adipose tissue concentrations of EC and measurements of body composition and insulin sensitivity observed here were similar to those observed in humans. These results underscore the strength of the non-human primate model in investigating pathways of energy metabolism that have relevance to human disease.

ACKNOWLEDGMENTS

We express our appreciation to the veterinarian technicians and the staff at the Texas Biomedical Research Institute (Texas Biomed) for their excellent care of the animals. In addition, we are grateful to Vicki Mattern at Texas Biomed and Sonya Veron, University of Texas Southwestern, for expert technical assistance, to Patricia Tramontanato, Raju Amin, and Yongi Lou (Sanofi) for discussions of the study design and measurements of plasma rimonabant, and to Dr. Franco Folli at the University of Texas Health Science Center at San Antonio for advice on data interpretation.

GRANTS

This study was funded by an unrestricted grant from Sanofi, and the investigation was conducted in facilities constructed with support from the Research Facilities Improvement Program under grant no. C06-RR (nos. 014578, 013556, 015456, and 017515) from the National Center for Research Resources, National Institutes of Health (NIH), and with support from NIH Grants PO1-HL-028972 and P51-RR-013986.

DISCLOSURES

The authors have no conflicts of interest, financial or otherwise, to declare. Portions of this work were presented at the American Diabetes Association National Meeting in Orlando, FL, 2010.

AUTHOR CONTRIBUTIONS

V.V., R.A.B., P.B.H., V.S.V., A.G.C., and E.J.P. did the conception and design of the research; V.V., R.A.B., P.B.H., V.S.V., S.K., and N.V.D. performed the experiments; V.V., R.A.B., and E.J.P. analyzed the data; V.V. and E.J.P. drafted the manuscript; R.A.B., S.K., N.V.D., D.P., and A.G.C. interpreted the results of the experiments; E.J.P. edited and revised the manuscript; E.J.P. approved the final version of the manuscript.

REFERENCES

1. **Annuzzi G, Piscitelli F, Di Marino L, Patti L, Giacco R, Costabile G, Bozzetto L, Riccardi G, Verde R, Petrosino S, Rivellese AA, Di Marzo V.** Differential alterations of the concentrations of endocannabinoids and related lipids in the subcutaneous adipose tissue of obese diabetic patients. *Lipids Health Dis* 9: 43, 2010.
2. **Barrows BR, Parks EJ.** Contributions of different fatty acid sources to very low-density lipoprotein-triacylglycerol in the fasted and fed states. *J Clin Endocrinol Metab* 91: 1446–1452, 2006.
3. **Barrows BR, Timlin MT, Parks EJ.** Spillover of dietary fatty acids and use of serum nonesterified fatty acids for the synthesis of VLDL-triacylglycerol under two different feeding regimens. *Diabetes* 54: 2668–2673, 2005.
4. **Bastarrachea RA, Veron SM, Vaidyanathan V, Garcia-Forey M, Voruganti VS, Higgins PB, Parks EJ.** Protocol for the measurement of fatty acid and glycerol turnover in vivo in baboons. *J Lipid Res* 52: 1272–1280, 2011.
5. **Bennetzen MF, Wellner N, Ahmed SS, Ahmed SM, Diep TA, Hansen HS, Richelsen B, Pedersen SB.** Investigations of the human endocannabinoid system in two subcutaneous adipose tissue depots in lean subjects and in obese subjects before and after weight loss. *Int J Obes (Lond)* 35: 1377–1384, 2011.
6. **Bensaid M, Gary-Bobo M, Esclangon A, Maffrand JP, Le Fur G, Oury-Donat F, Soubrié P.** The cannabinoid CB1 receptor antagonist SR141716 increases Acrp30 mRNA expression in adipose tissue of obese

fa/fa rats and in cultured adipocyte cells. *Mol Pharmacol* 63: 908–914, 2003.
7. **Bermudez-Silva FJ, Sanchez-Vera I, Suárez J, Serrano A, Fuentes E, Juan-Pico P, Nadal A, Rodríguez de Fonseca F.** Role of cannabinoid CB2 receptors in glucose homeostasis in rats. *Eur J Pharmacol* 565: 207–211, 2007.
8. **Bermúdez-Silva FJ, Suárez J, Baixeras E, Cobo N, Bautista D, Cuesta-Muñoz AL, Fuentes E, Juan-Pico P, Castro MJ, Milman G, Mechoulam R, Nadal A, Rodríguez de Fonseca F.** Presence of functional cannabinoid receptors in human endocrine pancreas. *Diabetologia* 51: 476–487, 2008.
9. **Bermúdez-Siva FJ, Serrano A, Diaz-Molina FJ, Sánchez Vera I, Juan-Pico P, Nadal A, Fuentes E, Rodríguez de Fonseca F.** Activation of cannabinoid CB1 receptors induces glucose intolerance in rats. *Eur J Pharmacol* 531: 282–284, 2006.
10. **Blüher M, Engeli S, Klöting N, Berndt J, Fasshauer M, Bátkai S, Pacher P, Schön MR, Jordan J, Stumvoll M.** Dysregulation of the peripheral and adipose tissue endocannabinoid system in human abdominal obesity. *Diabetes* 55: 3053–3060, 2006.
11. **Bordicchia M, Battistoni I, Mancinelli L, Giannini E, Refi G, Minardi D, Muzzonigro G, Mazzucchelli R, Montironi R, Piscitelli F, Petrosino S, Dessμ-Fulgheri P, Rappelli A, Di Marzo V, Sarzani R.** Cannabinoid CB1 receptor expression in relation to visceral adipose depots, endocannabinoid levels, microvascular damage, and the presence of the Cnr1 A3813G variant in humans. *Metabolism* 59: 734–741, 2010.
12. **Cavuoto P, McAinch AJ, Hatzinikolas G, Janovská A, Game P, Wittert GA.** The expression of receptors for endocannabinoids in human and rodent skeletal muscle. *Biochem Biophys Res Commun* 364: 105–110, 2007.
13. **Chavez AO, Gastaldelli A, Guardado-Mendoza R, Lopez-Alvarenga JC, Leland MM, Tejero ME, Sorice G, Casiraghi F, Davalli A, Bastarrachea RA, Comuzzie AG, DeFronzo RA, Folli F.** Predictive models of insulin resistance derived from simple morphometric and biochemical indices related to obesity and the metabolic syndrome in baboons. *Cardiovasc Diabetol* 8: 22, 2009.
14. **Chavez AO, Lopez-Alvarenga JC, Tejero ME, Triplitt C, Bastarrachea RA, Sriwijitkamol A, Tantiwong P, Voruganti VS, Musi N, Comuzzie AG, DeFronzo RA, Folli F.** Physiologic and molecular determinants of insulin action in the baboon. *Diabetes* 57: 899–908, 2008.
15. **Christopoulou FD, Kiortsis DN.** An overview of the metabolic effects of rimonabant in randomized controlled trials: potential for other cannabinoid 1 receptor blockers in obesity. *J Clin Pharm Ther* 36: 10–18, 2011.
16. **Coelho AMJ, Carey KD.** A social tethering system for nonhuman primates used in laboratory research. *Lab Anim Sci* 40: 388–394, 1990.
18. **Comuzzie AG, Cole SA, Martin L, Carey KD, Mahaney MC, Blangero J, VandeBerg JL.** The baboon as a nonhuman primate model for the study of the genetics of obesity. *Obes Res* 11: 75–80, 2003.
19. **Cota D, Marsicano G, Tschöp M, Grübler Y, Flachskamm C, Schubert M, Auer D, Yassouridis A, Thöne-Reineke C, Ortmann S, Tomassoni F, Cervino C, Nisoli E, Linthorst AC, Pasquali R, Lutz B, Stalla GK, Pagotto U.** The endogenous cannabinoid system affects energy balance via central orexigenic drive and peripheral lipogenesis. *J Clin Invest* 112: 423–431, 2003.
20. **Côté M, Matias I, Lemieux I, Petrosino S, Alméras N, Després JP, Di Marzo V.** Circulating endocannabinoid levels, abdominal adiposity and related cardiometabolic risk factors in obese men. *Int J Obes (Lond)* 31: 692–699, 2007.
21. **Di Marzo V, Verrijken A, Hakkarainen A, Petrosino S, Mertens I, Lundbom N, Piscitelli F, Westerbacka J, Soro-Paavonen A, Matias I, Van Gaal L, Taskinen MR.** Role of insulin as a negative regulator of plasma endocannabinoid levels in obese and nonobese subjects. *Eur J Endocrinol* 161: 715–722, 2009.
22. **DiPatrizio NV, Astarita G, Schwartz GP, Lic X, Piomellia D.** Endocannabinoid signal in the gut controls dietary fat intake. *Proc Natl Acad Sci USA* 108: 12904–12908, 2011.
23. **Donnelly KL, Smith CI, Schwarzenberg SJ, Jessurun J, Boldt MD, Parks EJ.** Sources of fatty acids stored in liver and secreted via lipoproteins in patients with nonalcoholic fatty liver disease. *J Clin Invest* 115: 1343–1351, 2005.
24. **Engeli S, Böhnke J, Feldpausch M, Gorzelniak K, Janke J, Bátkai S, Pacher P, Harvey-White J, Luft FC, Sharma AM, Jordan J.** Activation of the peripheral endocannabinoid system in human obesity. *Diabetes* 54: 2838–2843, 2005.
25. **Gasperi V, Fezza F, Pasquariello N, Bari M, Oddi S, Agrò AF, Maccarrone M.** Endocannabinoids in adipocytes during differentiation and their role in glucose uptake. *Cell Mol Life Sci* 64: 219–229, 2007.
26. **Giuffrida A, Rodríguez de Fonseca F, Piomelli D.** Quantification of bioactive acylethanolamides in rat plasma by electrospray mass spectrometry. *Anal Biochem* 280: 87–93, 2000.
27. **Guardado-Mendoza R, Davalli AM, Chavez AO, Hubbard GB, Dick EJ, Majluf-Cruz A, Tene-Perez CE, Goldschmidt L, Hart J, Perego C, Comuzzie AG, Tejero ME, Finzi G, Placidi C, La Rosa S, Capella C, Halff G, Gastaldelli A, DeFronzo RA, Folli F.** Pancreatic islet amyloidosis, beta-cell apoptosis, and alpha-cell proliferation are determinants of islet remodeling in type-2 diabetic baboons. *Proc Natl Acad Sci USA* 106: 13992–13997, 2009.
28. **Hellerstein MK, Neese RA.** Mass isotopomer distribution analysis at eight years: theoretical, analytic, and experimental considerations. *Am J Physiol Endocrinol Metab* 276: E1146–E1170, 1999.
29. **Herling AW, Kilp S, Elvert R, Haschke G, Kramer W.** Increased energy expenditure contributes more to the body weight-reducing effect of rimonabant than reduced food intake in candy-fed wistar rats. *Endocrinology* 149: 2557–2566, 2008.
30. **Hoareau L, Buyse M, Festy F, Ravanan P, Gonthier MP, Matias I, Petrosino S, Tallet F, d'Hellencourt CL, Cesari M, Di Marzo V, Roche R.** Anti-inflammatory effect of palmitoylethanolamide on human adipocytes. *Obesity* 17: 431–438, 2009.
31. **Jourdan T, Djaouti L, Demizieux L, Gresti J, Vergès B, Degrace P.** CB1 antagonism exerts specific molecular effects on visceral and subcutaneous fat and reverses liver steatosis in diet-induced obese mice. *Diabetes* 59: 926–934, 2010.
32. **Kamath S, Chavez AO, Gastaldelli A, Casiraghi F, Halff GA, Abrahamian GA, Davalli AM, Bastarrachea RA, Comuzzie AG, Guardado-Mendoza R, Jimenez-Ceja LM, Mattern V, Paez AM, Ricotti A, Tejero ME, Higgins PB, Rodriguez-Sanchez IP, Tripathy D, DeFronzo RA, Dick EJ Jr, Cline GW, Folli F.** Coordinated defects in hepatic long chain fatty acid metabolism and triglyceride accumulation contribute to insulin resistance in non-human primates. *PloS One* 6: e27617, 2011.
33. **Kleiber M.** *The Fire of Life: An Introduction to Animal Energetics*. Malabar, FL: Robert E. Krieger Publishing, 1987.
34. **Klein S, Young VR, Blackburn GL, Bistran BR, Wolfe RR.** Palmitate and glycerol kinetics during brief starvation in normal weight young adult and elderly subjects. *J Clin Invest* 78: 928–933, 1986.
35. **Kola B, Hubina E, Tucci SA, Kirkham TC, Garcia EA, Mitchell SE, Williams LM, Hawley SA, Hardie DG, Grossman AB, Korbonits M.** Cannabinoids and ghrelin have both central and peripheral metabolic and cardiac effects via AMP-activated protein kinase. *J Biol Chem* 280: 25196–25201, 2005.
36. **Matias I, Gonthier MP, Orlando P, Martiadis V, De Petrocellis L, Cervino C, Petrosino S, Hoareau L, Festy F, Pasquali R, Roche R, Maj M, Pagotto U, Monteleone P, Di Marzo V.** Regulation, function, and dysregulation of endocannabinoids in models of adipose and beta-pancreatic cells and in obesity and hyperglycemia. *J Clin Endocrinol Metab* 91: 3171–3180, 2006.
37. **Matias I, Gonthier MP, Petrosino S, Docimo L, Capasso R, Hoareau L, Monteleone P, Roche R, Izzo AA, Di Marzo V.** Role and regulation of acylethanolamides in energy balance: focus on adipocytes and beta-cells. *Br J Pharmacol* 152: 676–690, 2007.
38. **Moon JH, Kim HJ, Kim SK, Kang ES, Lee BW, Ahn CW, Lee HC, Cha BS.** Fat redistribution preferentially reflects the anti-inflammatory benefits of pioglitazone treatment. *Metabolism* 60: 165–172, 2011.
39. **Motaghedi R, McGraw TE.** The CB1 endocannabinoid system modulates adipocyte insulin sensitivity. *Obesity (Silver Spring)* 16: 1727–1734, 2008.
39a. **National Research Council.** Chapter 11. *Nutrient Requirements of Nonhuman Primates* (2nd revised ed.). Washington, DC: National Academies Press, 2003, p. 191–194.
39b. **Nogueiras R, Diaz-Arteaga A, Lockie SH, Velásquez DA, Tschop J, López M, Cadwell CC, Diéguez C, Tschöp MH.** The endocannabinoid system: role in glucose and energy metabolism. *Pharmacol Res* 60: 93–98, 2009.
40. **Nogueiras R, Veyrat-Durebex C, Suchanek PM, Klein M, Tschöp J, Caldwell C, Woods SC, Wittmann G, Watanabe M, Liposits Z, Fekete C, Reizes O, Rohner-Jeanrenaud F, Tschöp MH.** Peripheral, but not central, CB1 antagonism provides food intake-independent metabolic benefits in diet-induced obese rats. *Diabetes* 57: 2977–2991, 2008.

41. **Osei-Hyiaman D, DePetrillo M, Pacher P, Liu J, Radaeva S, Batkai S, Harvey-White J, Mackie K, Offertaler L, Wang L, Kunos G.** Endocannabinoid activation at hepatic CB1 receptors stimulates fatty acid synthesis and contributes to diet-induced obesity. *J Clin Invest* 115: 1298–1305, 2005.
42. **Osei-Hyiaman D, Liu J, Zhou L, Godlewski G, Harvey-White J, Jeong WI, Bátkai S, Marsicano G, Lutz B, Buettner C, Kunos G.** Hepatic CB1 receptor is required for development of diet-induced steatosis, dyslipidemia, and insulin and leptin resistance in mice. *J Clin Invest* 118: 3160–3169, 2008.
43. **Pagano C, Pilon C, Calcagno A, Urbanet R, Rossato M, Milan G, Bianchi K, Rizzuto R, Bernante P, Federspil G, Vettor R.** The endogenous cannabinoid system stimulates glucose uptake in human fat cells via phosphatidylinositol 3-kinase and calcium-dependent mechanisms. *J Clin Endocrinol Metab* 92: 4810–4819, 2007.
44. **Pagano C, Rossato M, Vettor R.** Endocannabinoids, adipose tissue and lipid metabolism. *J Neuroendocrinol* 20: 124–129, 2008.
45. **Parks EJ, Krauss RM, Christiansen MP, Neese RA, Hellerstein MK.** Effects of a low-fat, high-carbohydrate diet on VLDL-triglyceride assembly, production, and clearance. *J Clin Invest* 104: 1087–1096, 1999.
46. **Pavon FJ, Bilbao A, Hernández-Folgado L, Cippitelli A, Jagerovic N, Abellán G, Rodríguez-Franco MA, Serrano A, Macias M, Gómez R, Navarro M, Goya P, Rodríguez de Fonseca F.** Antiobesity effects of the novel in vivo neutral cannabinoid receptor antagonist 5-(4-chlorophenyl)-1-(2,4-dichlorophenyl)-3-hexyl-1H-1,2,4-triazole—LH 21. *Neuropharmacology* 51: 358–366, 2006.
47. **Pavón FJ, Serrano A, Pérez-Valero V, Jagerovic N, Hernández-Folgado L, Bermúdez-Silva FJ, Macías M, Goya P, de Fonseca FR.** Central versus peripheral antagonism of cannabinoid CB1 receptor in obesity: effects of LH-21, a peripherally acting neutral cannabinoid receptor antagonist, in Zucker rats. *J Neuroendocrinol* 20, *Suppl* 1: 116–123, 2008.
48. **Peter A, Cegan A, Wagner S, Lehmann R, Stefan N, Königsrainer A, Königsrainer I, Häring HU, Schleicher E.** Hepatic lipid composition and stearoyl-coenzyme A desaturase 1 mRNA expression can be estimated from plasma VLDL fatty acid ratios. *Clin Chem* 55: 2113–2120, 2009.
49. **Poirier B, Bidouard JP, Cadrouvele C, Marniquet X, Staels B, O'Connor SE, Janiak P, Herbert JM.** The anti-obesity effect of rimonabant is associated with an improved serum lipid profile. *Diabetes* 7: 65–72, 2005.
50. **Richey JM, Woolcott OO, Stefanovski D, Harrison LN, Zheng D, Lottati M, Hsu IR, Kim SP, Kabir M, Catalano KJ, Chiu JD, Ionut V, Kolka C, Mooradian V, Bergman RN.** Rimonabant prevents additional accumulation of visceral and subcutaneous fat during high-fat feeding in dogs. *Am J Physiol Endocrinol Metab* 296: E1311–E1318, 2009.
51. **Roche R, Hoareau L, Bes-Houtmann S, Gonthier M, Laborde C, Baron J, Haffaf Y, Cesari M, Festy F.** Presence of the cannabinoid receptors, CB1 and CB2, in human omental and subcutaneous adipocytes. *Histochem Cell Biol* 126: 177–187, 2006.
53. **Ruby MA, Nomura DK, Hudak CS, Mangravite LM, Chiu S, Casida JE, Krauss RM.** Overactive endocannabinoid signaling impairs apolipoprotein E-mediated clearance of triglyceride-rich lipoproteins. *Proc Natl Acad Sci USA* 105: 14561–14566, 2008.
54. **Schwarz JM, Linfoot P, Dare D, Aghajanian K.** Hepatic de novo lipogenesis in normoinsulinemic and hyperinsulinemic subjects consuming high-fat, low-carbohydrate and low-fat, high-carbohydrate isoenergetic diets. *Am J Clin Nutr* 77: 43–50, 2003.
55. **Schwarz JM, Neese RA, Turner S, Dare D, Hellerstein MK.** Short-term alterations in carbohydrate energy intake in humans. Striking effects on hepatic glucose production, de novo lipogenesis, lipolysis, and whole-body fuel selection. *J Clin Invest* 96: 2735–2743, 1995.
56. **Serrano A, Pavón FJ, Tovar S, Casanueva F, Señarís R, Diéguez C, de Fonseca FR.** Oleoylethanolamide: effects on hypothalamic transmitters and gut peptides regulating food intake. *Neuropharmacology* 60: 593–601, 2011.
57. **Shadid S, Jensen MD.** Effects of pioglitazone versus diet and exercise on metabolic health and fat distribution in upper body obesity. *Diabetes Care* 26: 3146–3152, 2003.
58. **Silvestri C, Ligresti A, Di Marzo V.** Peripheral effects of the endocannabinoid system in energy homeostasis: adipose tissue, liver and skeletal muscle. *Rev Endocr Metab Disord* 12: 153–162, 2011.
59. **Son MH, Kim HD, Chae YN, Kim MK, Shin CY, Ahn GJ, Choi SH, Yang EK, Park KJ, Chae HW, Moon HS, Kim SH, Shin YG, Yoon SH.** Peripherally acting CB1-receptor antagonist: the relative importance of central and peripheral CB1 receptors in adiposity control. *Int J Obes* 34: 547–556, 2010.
60. **Sunehag AL, Treuth MS, Toffolo G, Butte NF, Cobelli C, Bier DM, Haymond MW.** Glucose production, gluconeogenesis, and insulin sensitivity in children and adolescents: an evaluation of their reproducibility. *Pediatr Res* 50: 115–123, 2001.
61. **Tam J, Vemuri VK, Liu J, Bátkai S, Mukhopadhyay B, Godlewski G, Osei-Hyiaman D, Ohnuma S, Ambudkar SV, Pickel J, Makriyannis A, Kunos G.** Peripheral CB1 cannabinoid receptor blockade improves cardiometabolic risk in mouse models of obesity. *J Clin Invest* 120: 2953–2966, 2010.
62. **Timlin MT, Barrows BR, Parks EJ.** Increased dietary substrate delivery alters hepatic fatty acid recycling in healthy men. *Diabetes* 54: 2694–2701, 2005.
63. **Timlin MT, Parks EJ.** Temporal pattern of de novo lipogenesis in the postprandial state in healthy men. *Am J Clin Nutr* 81: 35–42, 2005.
64. **Triay J, Mundi M, Klein S, Toledo FG, Smith SR, Abu-Lebdeh H, Jensen M.** Does rimonabant independently affect free fatty acid and glucose metabolism? *J Clin Endocrinol Metab* 97: 819–827, 2012.
65. **Westerbacka J, Lammi K, Hakkinen AM, Rissanen AM, Salminen I, Aro A, Yki-Jarvinen H.** Dietary fat content modifies liver fat in overweight nondiabetic subjects. *J Clin Endocrinol Metab* 90: 2804–2809, 2005.
66. **Yin W, Carballo-Jane E, McLaren DG, Mendoza VH, Gagen K, Geoghagen NS, McNamara LA, Gorski JN, Eiermann GJ, Petrov A, Wolff M, Tong X, Wilsie LC, Akiyama TE, Chen J, Thankappan A, Xue J, Ping X, Andrews G, Wickham LA, Gai CL, Trinh T, Kulick AA, Donnelly MJ, Voronin GO, Rosa R, Cumiskey AM, Bekkari K, Mitnaul LJ, Puig O, Chen F, Raubertas R, Wong PH, Hansen BC, Koblan KS, Roddy TP, Hubbard BK, Strack AM.** Plasma lipid profiling across species for the identification of optimal animal models of human dyslipidemia. *J Lipid Res* 53: 51–65, 2012.